BMC Medical Genomics

RESEARCH

Open Access

Nanopore-based full-length transcriptome sequencing for understanding the underlying molecular mechanisms of rapid and slow progression of diabetes nephropathy

Jing E[1,2†], Shun-Yao Liu[6†], Dan-Na Ma[1,2†], Guo-Qing Zhang[1,3], Shi-Lu Cao[7], Bo Li[1,2], Xiao-hua Lu[1], Hong-Yan Luo[1], Li Bao[1], Xiao-Mei Lan[2,4], Rong-Guo Fu[5*] and Ya-Li Zheng[1*]

Abstract

Background Diabetic nephropathy (DN) has been a major factor in the outbreak of end-stage renal disease for decades. As the underlying mechanisms of DN development remains unclear, there is no ideal methods for the diagnosis and therapy.

Objective We aimed to explore the key genes and pathways that affect the rate progression of DN.

Methods Nanopore-based full-length transcriptome sequencing was performed with serum samples from DN patients with slow progression (DNSP, $n=5$) and rapid progression (DNRP, $n=6$).

Results Here, transcriptome proclaimed 22,682 novel transcripts and obtained 45,808 simple sequence repeats, 1,815 transcription factors, 5,993 complete open reading frames, and 1,050 novel lncRNA from the novel transcripts. Moreover, a total of 341 differentially expressed transcripts (DETs) and 456 differentially expressed genes (DEGs) between the DNSP and DNRP groups were identified. Functional analyses showed that DETs mainly involved in ferroptosis-related pathways such as oxidative phosphorylation, iron ion binding, and mitophagy. Moreover, Functional analyses revealed that DEGs mainly involved in oxidative phosphorylation, lipid metabolism, ferroptosis, autophagy/mitophagy, apoptosis/necroptosis pathway.

Conclusion Collectively, our study provided a full-length transcriptome data source for the future DN research, and facilitate a deeper understanding of the molecular mechanisms underlying the differences in fast and slow progression of DN.

†E Jing, Shun-Yao Liu and Dan-Na Ma contributed equally to this work.

*Correspondence:
Rong-Guo Fu
pipifu@126.com
Ya-Li Zheng
zhengyali@nxmu.edu.cn

Full list of author information is available at the end of the article

Keywords Diabetic, Nephropathy full-length transcriptome, Ferroptosis, Autophagy/mitophagy, Apoptosis/necroptosis

Introduction

Diabetic nephropathy (DN) has been the main cause of end-stage renal disease (ESRD) for decades [1, 2]. The prevalence of DN is about 25–40% [3]. The number of diabetes patients has risen sharply. Meanwhile, the incidence rate and the number of DN patients have also increased significantly, and the clinical treatment, economic development, and social pressure have become increasingly heavy. At present, clinical treatment of DN mainly focuses on controlling glycemic levels, normalizing blood pressure, and blocking the renin–angiotensin–aldosterone system (RAAS) [4]. However, most of these treatments have side effects, and their curative effects are limited. Hence, there is an urgent need to explore the molecular mechanism of DN progression.

The pathogenesis of DN is a complex process, which involves multiple mechanisms and factors [5, 6]. Increasing evidence have found that inflammatory pathways play a crucial role in the pathogenesis of DN in recent years [7, 8]. It has been proved that proinflammatory cytokines are involved in the progress of DN, including interleukin-6 (IL-6), interleukin-10 (IL-10), and tumor necrosis factor-α (TNF-α) [9, 10]. Nevertheless, the specific mechanism regarding the disease progression of DN is still unclear. Therefore, it is urgent to find out the effective molecular targets and key signaling pathways involved in the disease progression of DN.

Oxford Nanopore Technologies (ONT) sequencing is a new generation single molecule real-time electrical signal sequencing technology based on nanopore [11]. The sequencing principle is to calculate the type of the corresponding base and complete the real-time determination of the sequence by detecting and corresponding the electrical signal [12, 13]. Transcriptome research could help us deeply understand life processes. However, traditional RNA-Seq2.0 technology cannot exactly provide or assemble complete transcripts, and can no longer keep up with the rapid development of bioinformatics. Conversely, ONT-based full-length transcriptome sequencing does not need to interrupt RNA fragments, and full-length cDNA is obtained by reverse transcription. The ultra-long reading of the platform contains the sequence information of a single complete transcript, and the later analysis does not require assembly, and the result is what is measured [12]. Therefore, the main advantages of ONT are real-time sequence analysis, ultra-long read length, high-fidelity, and base modification detection allowed. There are already some studies using ONT technology to resolve disease progression. For example, Xue et al. used full-length transcriptome sequencing to analyze differentially expressed genes and signaling pathways related to oxymatrine treatment of psoriasis [14]. The full-length transcriptome data obtained by Oehler et al. revealed that transcriptional regulation and alternative splicing may influence PGC-1α function expression in injured and metabolically challenged hearts [15]. However, there are no relevant reports exploring the rapidity of DN progression based on ONT.

In this study, aim to deeply understand the regulatory mechanism of DN progress, we used the ONT sequencing method to obtain full-length transcriptome in serums of DN patients with slow progression (DNSP, 5 samples) and rapid progression (DNRP, 6 samples). Next, we further analyzed the differentially expressed transcripts (DETs) and differentially expressed genes (DEGs) in DNSP and DNRP groups, and revealed the key signaling pathways that promote rapid progression of DN. These results are expected to provide a new direction for studying the molecular mechanism of the rapid progression of DN in the future.

Materials and methods

Clinical samples

Whole blood (20 mL) was drawn from 11 patients, including 5 cases in the DNSP group and 6 cases in the DNRP group. The detailed clinical information of patients is presented in Table 1.

Currently, there are no detailed clinical diagnostic criteria for DN patients with rapid and slow progression in various clinical nephropathy guidelines and uptodate. We have found in clinical practice that the onset of DN is not necessarily related to the history of diabetes, nor to the control of blood sugar levels. Some patients may have a history of diabetes for more than 20 years without cumulative kidney damage, while others may be newly diagnosed with diabetes and already exhibit kidney involvement with rapid disease progression. Therefore, our study classified patients into two groups (DNSP and DNRP), based on the clinical history of diabetes, laboratory tests, and complications. Inclusion criteria: (1) Patients aged 18–80 years with a definite diagnosis of diabetes. (2) The DNSP group is the patients with diabetes for more than 20 years, without DN or only with urinary microalbumin, which has been maintained for a long time. (3) The DNRP patients have a history of diabetes for less than 10 years and have been clearly diagnosed as clinical stage IV of DN (characterized by significant proteinuria) through kidney biopsy or rapidly progressing to end-stage renal disease. The kidney biopsy pathology revealed stage IIb or III glomerular lesions. (4) Not using

Table 1 The detailed clinical information of patients

Group	Age	Diagnosis	Fundus complications	Drugs	HbA1c level (%)	History of diabetes	Renal biopsy findings	eGFR (mL/min)	Albuminuria	4-hour urine protein quantification (mg/24 h)
DNRP	64*	Clinical stage IV of DN	Diabetic retinopathy	Medicinal charcoal, alprostadil, Chinese medicine Shenshuaining	6.9	2 years	Stage III of DN	21.71	3+	5992
	55*	Clinical stage IV of DN	Hypertensive fundus disease	Tripterygium, irbesartan	7.6	4 years	Stage III of DN	34.1	3+	4120
	32	Clinical stage IV of DN	Diabetic retinopathy	Tripterygium, irbesartan	5.3	5 years	Stage III of DN	55.91	3+	9693
	57	Clinical stage IV of DN	Optic atrophy	Benazepril, Chinese medicine Kunxian capsule	8	0 month	Stage IIb of DN	108.4	2+	2665
	35	Clinical stage IV of DN	Diabetic retinopathy	Tripterygium, irbesartan	8.7	9 years	Stage III of DN	47.04	4+	28646.5
	47	Clinical stage IV of DN	Diabetic retinopathy	Valsartan	10.9	5 years	Stage IIb of DN	68.52	3+	3557.5
DNSP	54*	Diabetes	Cataract	Dapagliflozin	11.3	26 years	-	138.54	-	79.2
	63*	Diabetes	No	No	9.7	25 years	-	130.05	-	37.4
	66	Diabetes	Diabetic retinopathy	Empagliflozin	7.7	21 years	-	89.47	-	80.1
	47	Diabetes	No	No	12.5	25 years	-	108.7	-	102.4
	78*	Diabetes	No	Empagliflozin	10.3	25 years	-	109.08	-	100.5

Note: All 11 samples were used for ONT sequencing and *labeled samples were used for qRT-PCR validation. In addition, to ensure the number of replicates ($n=3$), two of the DNRP samples were mixed as new sample for qRT-PCR

medications such as traditional Chinese medicine, non-steroidal anti-inflammatory drugs, and others known to cause kidney damage. (5) Complete data, regular follow-up in outpatient clinics. Exclusion criteria: (1) Patients with kidney biopsy showing concurrent other types of nephritis; (2) Patients with conditions such as congestive heart failure, liver cirrhosis, malignant hypertension, tumors, which promote the progression of kidney disease. Patients with uremia, that is patients diagnosed with stage 5 chronic kidney disease (CKD) according to the 2023 KDIGO CKD guidelines. Blood samples were stored at normal temperature for 2 h and centrifuged at 2500 rpm for about 15 min. Then serum was collected. Finally, we kept serum samples at -80 °C before use. Written informed consent of all patients was obtained for this study.

It needs to be clarified that nephropathy-related drugs were added after the patient was diagnosed with diabetic nephropathy after renal puncture, and blood samples were collected and sent for gene sequencing immediately after diabetic nephropathy, and there was little effect of drugs. In addition, Tripterygium wilfordii polyglucoside and Kunxian capsule are non-steroidal immunosuppressive agents, which can inhibit cell proliferation and induce cell apoptosis. Several studies in China have reported that these drugs can delay the progression of diabetic nephropathy [16–19]. Shenshuanning capsule is an original product developed in China. Its main ingredients include Radix pseudotumor, Pinellia, rhubarb and salvia miltiorrhiza, etc. It can be used in patients with chronic renal insufficiency and has the effect of relieving turbidity. Thus, these drugs had little effect on sample sequencing.

Library construction and sequencing

We prepared 1 μg total RNA for building cDNA libraries using cDNA-PCR Sequencing Kit (SQKLSK110+EXP-PCB096) provided by ONT. Full-length cDNA was richened in template switching activity by reverse transcriptase, and defined PCR adapters were added to both ends of the first strand of cDNA. Then, cDNA was subjected to PCR for 14 circles using LongAmp Tag (NEB), followed by the PCR products connected to ONT adaptor ligation with T4 DNA ligase (NEB). XP reagent beads were applied to DNA purification based on ONT instructions. Finally, the cDNA libraries were loaded on FLO-MIN109 flow cells and sequenced on PromethION platform (Biomarker Technology Company, Beijing, China).

ONT long read processing

First, we filtered raw reads with a minimum average read quality score=6 and minimum read length=350 bp. Ribosomal RNA was mapped to the rRNA database and

then discarded. Secondly, we identified full-length, non-chimeric transcripts by searching for primers at both ends of reads. Furthermore, we obtained consensus isoforms after polishing full-length sequences. Finally, we clarified transcript sequences by mapping consensus sequences to the reference genome using minimap2.

Structure analysis

Using gffcompare to confirm transcripts according to known reference transcript annotations. The AStalavista tool was used to determine alternative splicing (AS) events. Simple sequence repeat (SSR) was analyzed by multiple intelligent software agents (MISA) software. The coding sequence (CDS) was predicted using TransDecoder. Transcription factors (TF) were identified from the animal transcription factor binding site (TFDB).

LncRNA prediction

Using Coding Potential Calculator (CPC; http://cpc2.cbi.pku.edu.cn), Coding-Non-Coding Index (CNCI; https://github.com/www-bioinfo-org/CNCI), Coding Potential Assessment Tool (CPAT http://lilab.research.bcm.edu/cpat/), and Pfam (http://www.sanger.ac.uk/Software/Pfam/) calculation methods to determine non-protein coding RNA from hypothetical protein-coding RNAs in the transcripts. Next, we utilized minimum length and exon number threshold to remove hypothetical protein-coding RNAs. Besides, transcripts longer than 200 nt with more than two exons were identified as candidate lncRNA. Finally, CPC/CNCI/CPAT/Pfam were used to demonstrate the protein-coding genes from the non-coding genes.

DETs and DEGs analysis

Genes are the basic units that control the transmission of genetic information in an organism, while transcripts are the products of gene expression. Since several different transcripts of the same gene can exist at the same time, many reads can be perfectly matched to multiple transcripts at the same time. For the gene, full-length reads were mapped to the reference transcriptome sequence, and quantification of a gene by counting all transcripts of the gene as quantitative results of the gene. For the transcript, full-length reads were also mapped to the reference transcriptome sequence, and quantification of a transcript by counting all transcripts as quantitative results. Reads with a match quality greater than 5 were used for quantification. Then, we assessed the expression levels by mapping reads per gene/transcript per 10,000 reads. Differential expression analysis for DETs/DEGs of two groups was performed by the DESeq2 R package. DESeq2 provided statistical routines for determining differential expression in digital gene expression data using a model based on the negative binomial distribution. Using Benjamini and Hochberg's approach to adjust *P*-value. Genes with adjusted *P*-value <0.05 and fold change ≥ 1.5 were recognized DEGs. Transcripts with adjusted *P*-value <0.01 and fold change ≥ 1.5 were recognized DETs. R package pheatmap was applied to draw the clustered heatmap.

Functional enrichment analysis

Gene Ontology (GO) analysis was realized using the GOseq R packages based on Wallenius non-central hyper geometric distribution. Kyoto Encyclopedia of Genes and Genomes (KEGG) is a database resource that can help us better understand the advanced functions and uses of biological systems from molecular-level information. We detected the enrichment degree of DETs and DEGs in KEGG signaling pathways by KO-Based Annotation System (KOBAS) software. Moreover, Non-Redundant-Protein Sequence Database (NR; ftp://ftp.ncbi.nlm.nih.gov/blast/db), SwissProt (http://www.uniprot.org/uniprot/?query=*&fil=reviewed%3Ayes), Clusters of Orthologous Groups (COG; https://www.ncbi.nlm.nih.gov/COG/), Clusters of orthologous groups for eukaryotic complete genomes (KOG; http://www.ncbi.nlm.nih.gov/KOG/), Pfam, and Gene set enrichment analysis (GSEA; https://www.broadlnstitute.org/gsea/) were used to perform functional prediction analysis for all the novel transcripts, DETs, and DEGs.

Protein-protein interaction (PPI)

The sequences of the DEGs were blast (blastx) to the genome of a related species and then constructed the predicted PPI network of these DEGs based on the interaction pairs of homologous proteins in the STRING database (http://string-db.org/). Using Cytoscape to visualize the PPI network diagram.

Quantitative real-time PCR (qRT-PCR)

Total RNA was extracted from 6 serum samples (3 samples in each group) using Trizol and quantified by scandrop 100 (Analytik Jena AG, factories at Konrad-Zuse-Str.1, D-07745 Jena, Germany). Set 3 technical repetitions for each cell sample. Reverse transcription reaction was conducted by TransScript First-Strand cDNA Synthesis kit (AiDLAB Biotech, Beijing, China) to synthesize the first strand of cDNA. The qRT-PCR was performed on qTOWER 2.0/2.2 Quantitative Real-Time PCR Thermal Cyclers (Analytik Jena AG, factories at Konrad-Zuse-Str.1, D-07745 Jena, Germany) using 2×SYBR® Green Master Mix (DF Biotech., CHENGDU, China). Primers were designed by Beacon Designer 7.9 and shown in Additional file 1. GAPDH served as an internal control gene. The relative gene expression was calculated by the qPCRsoft3.2 software automatically using the Pfaffl method [20].

Statistical analysis

The data analysis of qRT-PCR was carried out using GraphPad Prism 9.0. Before data analysis, both normality of the distribution and homogeneity of variance were assessed. A t-test was applied for comparing differences between the two groups and p less than 0.05 was considered statistically significant.

Results

Overview the full-length sequences

In our initial analysis of the clinical data, we observed no significant differences in age and glycated hemoglobin (HbA1c) levels between the DNRP and DNSP groups (Fig. 1). However, a notable difference was observed in the estimated glomerular filtration rate (eGFR) (Fig. 1). In our research, full-length transcriptome sequencing was performed in 11 serum samples from 5 DNSP and 6 DNRP patients, and the clean data of each sample reached 3.16 GB. The number of full-length sequences per sample ranged from 3,036,243 to 6,512,168. Another, we mapped consensus isoform to the reference genome using minimap2 and dislodged redundancy. Eventually, we determined common 46,250 non-redundant transcript sequences. We compared the redundancy of all samples with the definitive reference genome annotations, and then we found 12,720 new gene loci and 22,682 novel transcripts.

Functional annotation of novel transcripts

All the novel transcripts were mapped to seven databases: NR, SwissProt, GO, COG, KOG, Pfam, and KEGG, then we obtained functional annotation information of novel transcripts. A total of 15,121 isoforms were annotated. Furthermore, 9,515 isoforms were annotated in the

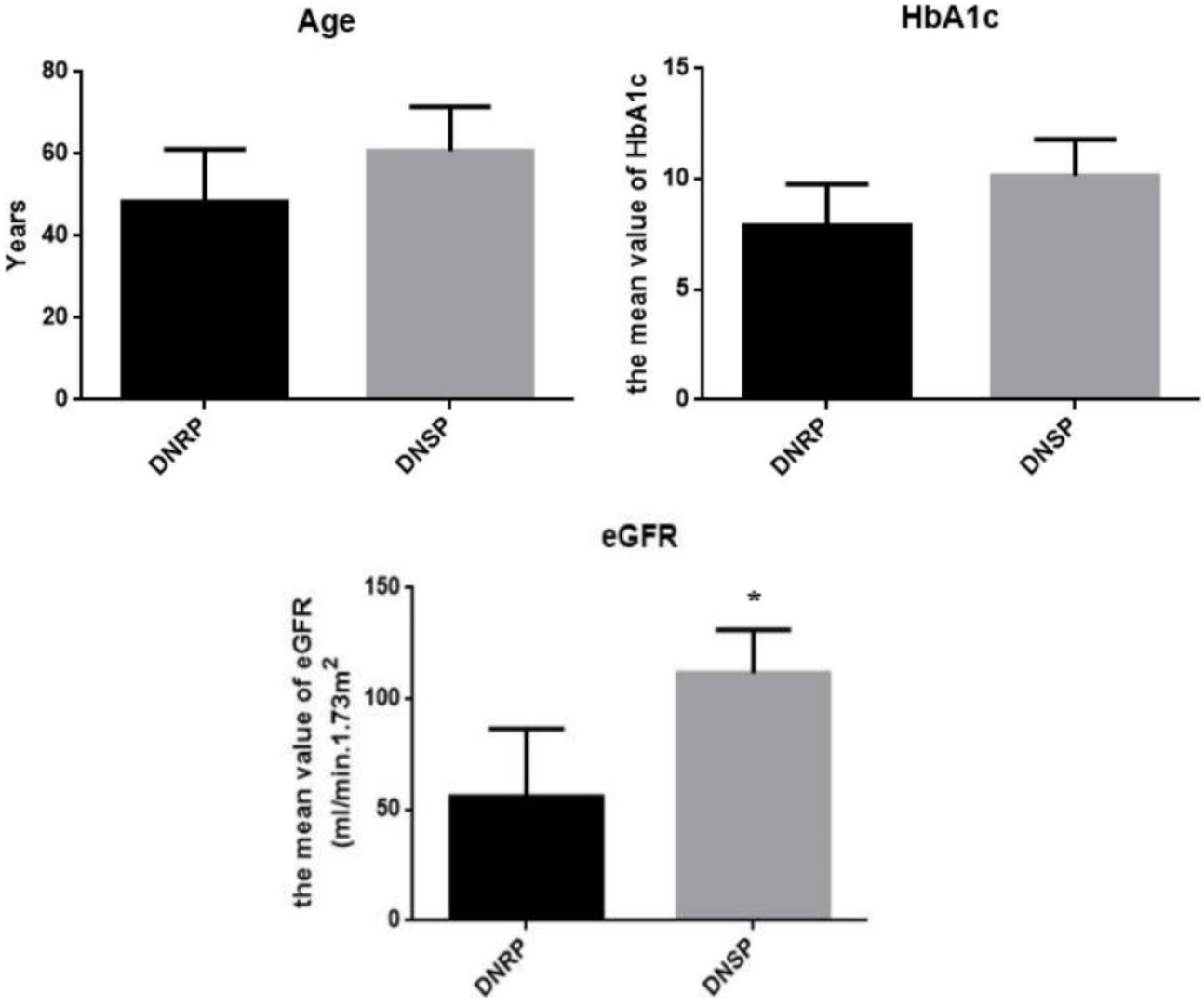

Fig. 1 Differences in clinical data of age, glycated hemoglobin (HbA1c) levels and the estimated glomerular filtration rate (eGFR) between DNRP and DNSP groups

GO database and 11,020 isoforms were annotated in the KEGG database. The NR database had the largest number of isoform annotations, a total of 14,832. Conversely, the COG database had only 1,242 isoforms, which was the least (Additional file 2).

SSR and TF analysis

Transcripts with more than 500 bp were screened from the transcripts after redundancy removal, and SSR analysis was carried out using MISA software. A total number of 107,610 sequences and a total size of 226,675,191 bp were detected by SSR analysis. Our result indicated that the total number of identified SSRs was 45,808, and the number of SSR containing sequences was 25,698 (Additional file 3). Seven types of SSRs were identified, including Mono-nucleotide, Di-nucleotide, Tri-nucleotide, Tetra-nucleotide, Penta-nucleotide, Hexa-nucleotide, and compound SSR. The number of Mono-nucleotide was the highest (26,386), and the number of Hexa-nucleotide was the lowest (80) (Additional file 3, Fig. 2A).

Besides, the identification of animal TF predicted common 1,815 TFs in the new transcripts. The main TF types were zi-C2H2, Homeobox, bHLH, HMG, ZBTB, TF_bZIP, Fork_head, ETS, MYB, IRF, zi-CCCH, THR-like, T-box, zi-GATA, Pou, THAP, SAND, RXR-like, and E2F. Among them, zi-C2H2 is the most TFs, while E2F is the least (Fig. 2B).

CDS and lncRNA prediction

TransDecoder software was used to predict the coding region sequence and its corresponding amino acid sequence of the novel transcript. A total of 12,128 ORFs were obtained, including 5,993 complete ORFs. The number of complete ORFs in the 0–100 aa section was the largest. As the length increased, the number of complete ORFs decreased (Fig. 2C). Moreover, we predicted 1,050 lncRNA transcripts using CPC, CNCI, CPAT, and Pfam methods (Fig. 2D). All identified lncRNAs were subdivided into the following four types: lincRNAs (long intergenic noncoding RNAs, 568, 54.1%), antisense-lncRNAs (209, 19.9%), intronic-lncRNAs (188, 17.9%), and sense-lncRNAs (85, 8.1%) (Fig. 2E). Ferroptosis has been reported to involve in DN progression [21]. We found that lncRNA ONT.3784.1 was targeted to SLC7A11, a ferroptosis marker gene [22], so we speculated that lncRNA ONT.3784.1 may affect the rate of process of DN by targeting SLC7A11 to regulate ferroptosis.

Identification, annotation and PPI network analysis of DETs

The number of DETs in the DNSP and DNRP comparison was 341, including 87 up-regulated transcripts and 254 down-regulated transcripts (Fig. 3A, Additional file 4). Cluster heatmap could more intuitively observe the difference in DETs expression level between groups (Fig. 3B). To further identify the functional annotation of DETs, we performed GO, KEGG, and GSEA analysis. We found that the DETs were primarily enriched in the GO category of molecular function regulator and antioxidant activity (Fig. 4A). Furthermore, the DETs mainly enriched in oxidative phosphorylation, mitophagy, and primary immunodeficiency in the KEGG database (Fig. 4B). As shown in Fig. 4C, GSEA analysis of DETs discovered that DETs distributed in the process of oxidative phosphorylation and iron ion binding. Interestingly, signaling pathways such as oxidative phosphorylation, iron ion binding, and mitophagy are all closely associated with ferroptosis [23]. Therefore, we conjectured that ferroptosis may be one of the mechanisms by which DETs determine the rate of DN progression.

To explore the interactions among proteins in DNSP vs. DNRP, we constructed a PPI network diagram based on DETs. The gene regulatory relationship of DN progression can be quickly identified by network structure analysis. Here, the nodes with the largest number of edges were supposed to be potential key genes, for example, HBB-206, CD163-209, HBA1-201, HSPA1A, and AHSP-201 were the most remarkable node genes (Fig. 4D). The PPI also suggested that many novel transcripts also play a central role in the DN progression, such as ONT.4235 and ONT.8261 cluster (Fig. 4D).

Identification and functional profiles of DEGs

Furthermore, we determined a total of 456 DEGs in the DNRP group compared with the DNSP group, including 141 up-regulated DEGs and 315 down-regulated DEGs (Fig. 5A, Additional file 5). Interestingly, we found that the previously mentioned TF, E2F, which is also in the list of DEGs, had a significantly lower expression level in the DNRP group than in the DNSP group (Additional file 5). Heatmap cluster analysis was also conducted on DEGs (Fig. 5B). To further identify the functional annotation of DEGs, we performed GO, KEGG, COG, and eggNOG analysis. We found that the DEGs were primarily enriched in the GO category of metabolic process, molecular function regulator, and antioxidant activity (Fig. 6A). Moreover, DEGs were mainly involved in the pathways of oxidative phosphorylation and sphingolipid metabolism (Fig. 6B). In the COG database, the DEGs were significantly enriched in lipid transport and metabolism, inorganic ion transport and metabolism (Fig. 6C). Similarly, in the eggNOG database, DEGs were also significantly enriched in lipid transport and metabolism (Fig. 6D). Together, the analysis of DEGs enrichment in GO, KEGG, COG, and eggNOG showed certain consistency and correlation, we hypothesized that DEGs may be involved in the progression rate of DN by affecting lipid metabolism and oxidative phosphorylation.

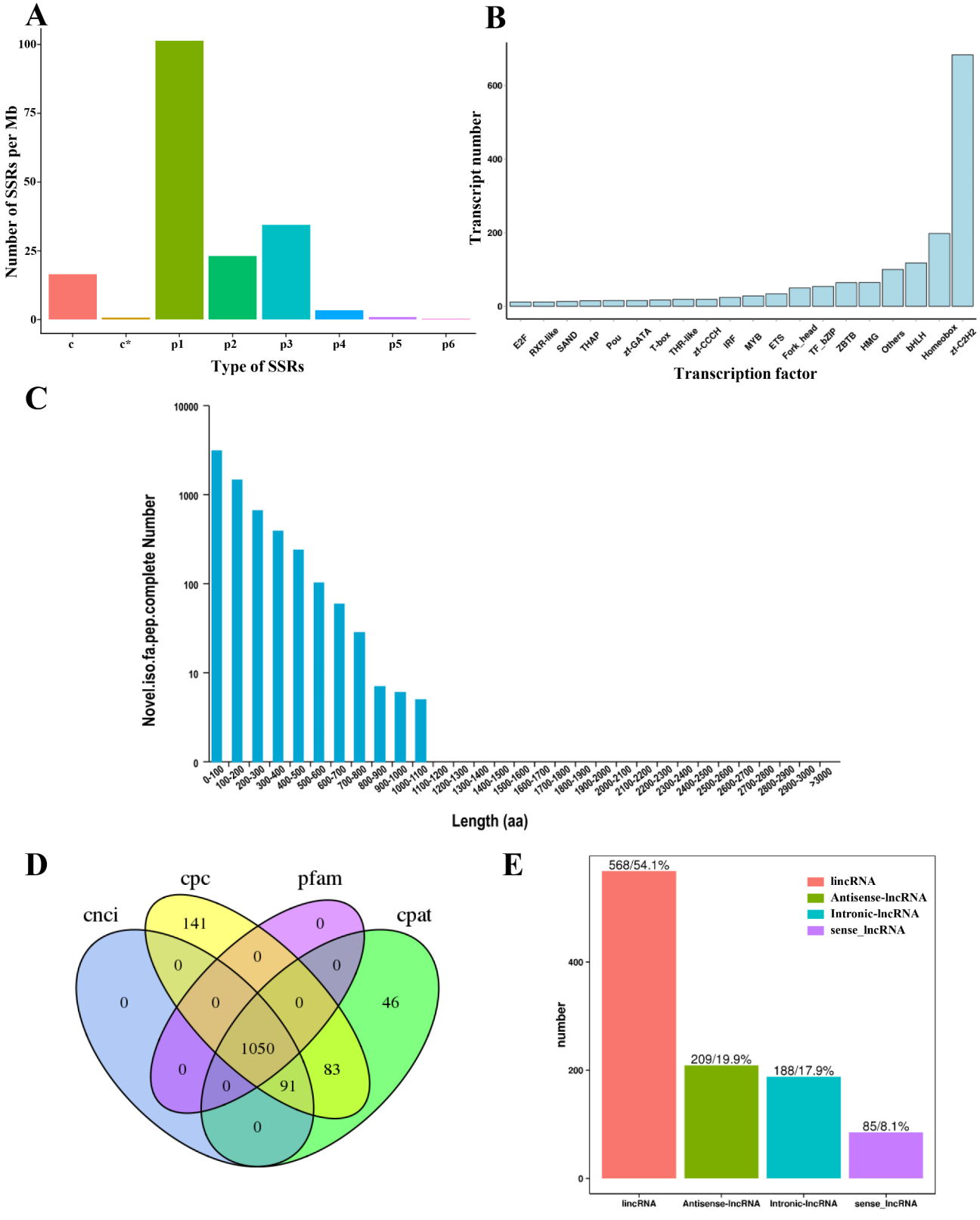

Fig. 2 The structural analysis of novel transcripts. **A** The type distribution of SSR. **B** The type distribution of TF. **C** Length distribution of CDS of complete ORFs. **D** Venn diagram of lncRNA transcripts were verified by CPC, CNCI, CPAT, and Pfam databases. **E** The type classification of lncRNAs

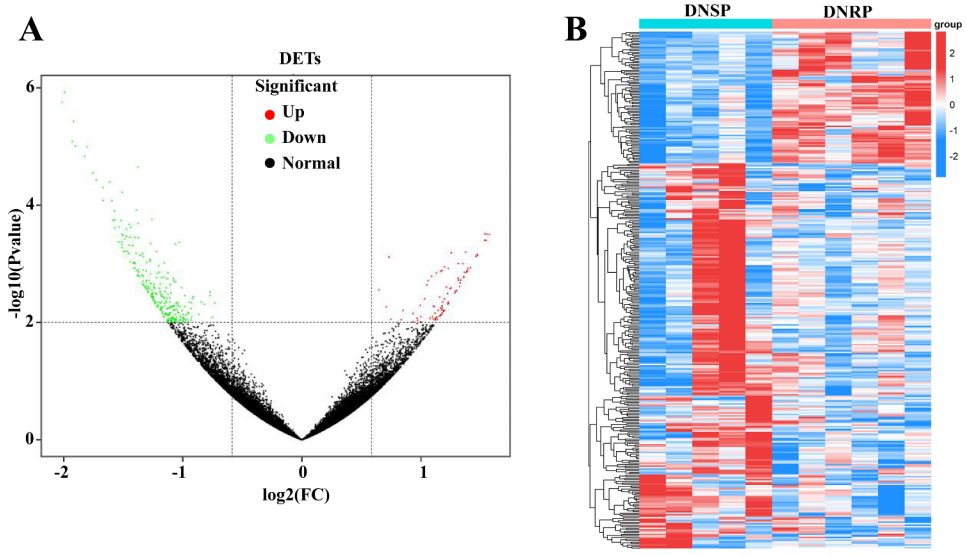

Fig. 3 Differential expression of transcripts in DNSP vs. DNRP. **A** Volcanic plot of the DETs. Red: up-regulated; Green: down-regulated; Black: normal. The y axis shows the -log10(*P*- adjusted value). **B** Cluster heatmap of the DETs

Ferroptosis related DEGs are involved in DN process

As recently reported that ferroptosis was involved in DN progression [21]. In this study, using ferroptosis database FerrDb V2 (http://www.zhounan.org/ferrdb/current/), we identified 33 ferroptosis-related DEGs, including MMD, ZEB1, PCBP1, and NF2 (Fig. 7). These ferroptosis-related DEGs were mainly involved in MAPK signaling pathway, ferroptosis pathway, oxidative phosphorylation, PI3K-Akt signaling pathway, glutathione metabolism, and p53 signaling pathway. Compared with the DNSP group, most ferroptosis-related DEGs were down-regulated in the DNRP group (Fig. 7). Moreover, interestingly, 7 DEGs in the SLC family were identified (Additional file 4), including SLC4A1, SLC38A5, SLC25A40, SLC12A7, SLC16A7, SLC35E1, and SLC47A1. Therefore, these data further demonstrated that ferroptosis plays a role in the rate of progression of DN.

Autophagy/mitophagy pathway are involved in DN progression

There were reports in the literature suggesting that autophagy affects DN progression by targeting mTOR signaling pathway [24, 25]. Likewise, in our KEGG enrichment results, DEGs were found involved in autophagy, mitophagy, and mTOR signaling pathway, which was displayed by the network plot. The DEGs enriched in mitophagy were BNIP3L [26], RRAS2, UBB, UBA52, and ONT.15,763. The mTOR signaling pathway enriched DEGs include STRADB, MIOS, ONT.18,929, ONT.21,457, and ONT.670. Moreover, autophagy-enriched DEGs were IGBP1, PPP2CA, PIK3R4, RB1CC1 [27], RRAS2, MAP3K7CL, ONT.15,763, ONT.18,929, and ONT.8101 (Fig. 8). Together, autophagy/mitophagy is involved in the rate of DN progression.

Apoptosis/necroptosis pathway are involved in DN progression

The involvement of apoptosis in the pathogenesis of DN has also been reported in previous studies [28]. Hence, we further uncovered the DEGs in the apoptosis/necroptosis pathway associated with the rate of DN progression. According to the results of KEGG, only ONT.18,929 and ONT.3200 were annotated into the apoptosis pathway. Moreover, The DEGs annotated to the necroptosis pathway include H2AFV, CAMK2D, NLRP3 [29] and ONT.8101 (Table 2). Therefore, these DEGs may be key genes in the rate of DN progression affected by apoptosis/necroptosis.

Validation by GSE142025 dataset and qRT-PCR

To validate the sequencing results of this study, we searched the GEO database (https://www.ncbi.nlm.nih.gov/geo/) for "diabetic nephropathy", expectedly, there were no transcriptomic data consistent with the design of this study protocol (comparison of the DNSP and DNRP groups), and as a result, the GSE142025 dataset was selected for analysis and comparison. The GSE142025 dataset contains transcriptomic data from patients with early and advanced DN. Compared with early DN patients, a total of 1765 genes were differentially expressed in the advanced DN group (Fig. 9A). Only 32 DEGs overlapped in our ONT sequencing and GSE142025 dataset (Fig. 9B). Interestingly, KEGG enrichment showed that these DEGs in the GSE142025 dataset were also involved in oxidative phosphorylation, sphingolipid metabolism, ferroptosis, apoptosis, and necroptosis pathways (Fig. 9C), which was consistent with our results.

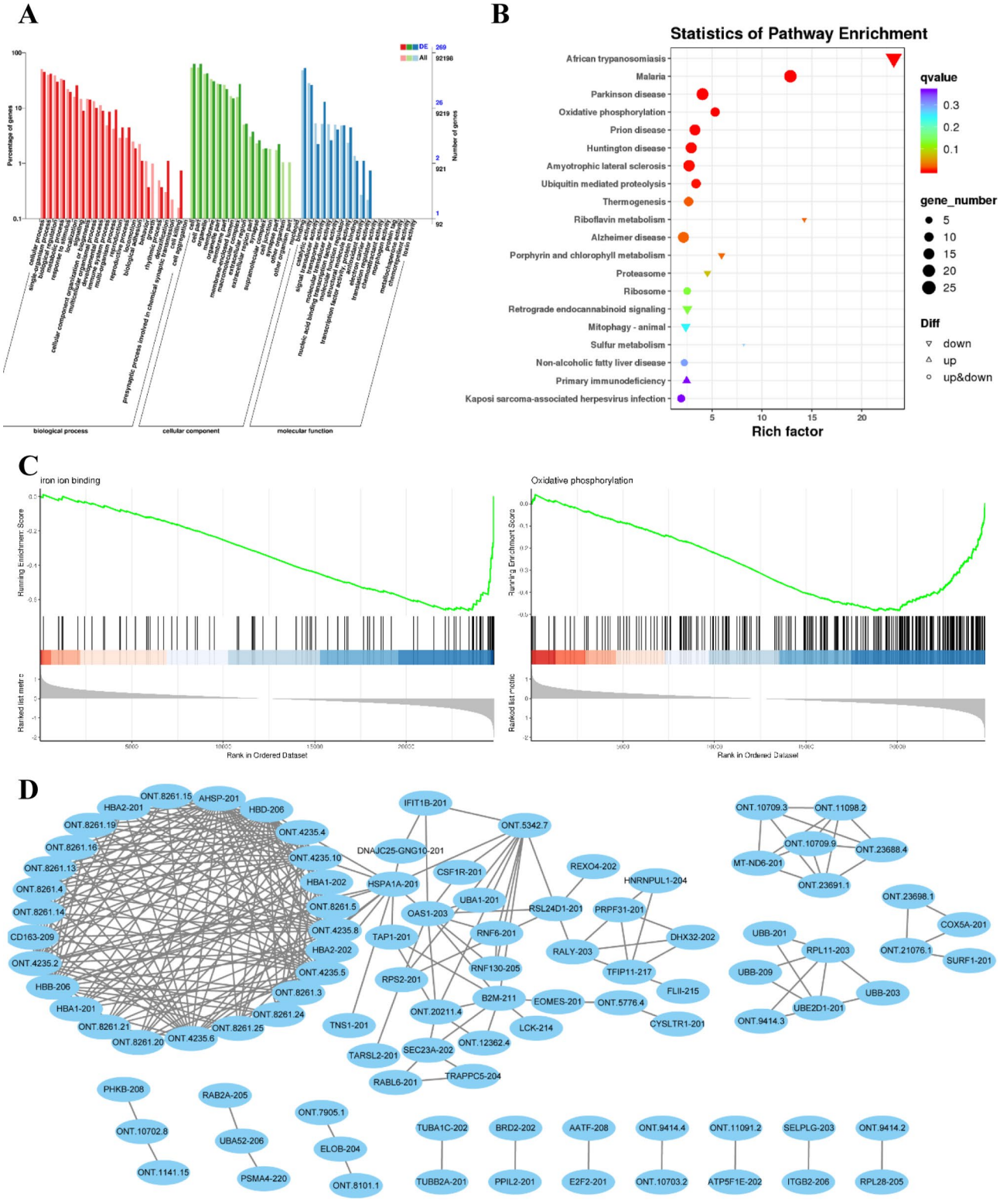

Fig. 4 Functional annotation of DETs. **A** Annotation of GO function. **B** Bubble plot of KEGG signaling pathway enrichment. **C** Annotation of GSEA function. **D** PPI network analysis of DETs

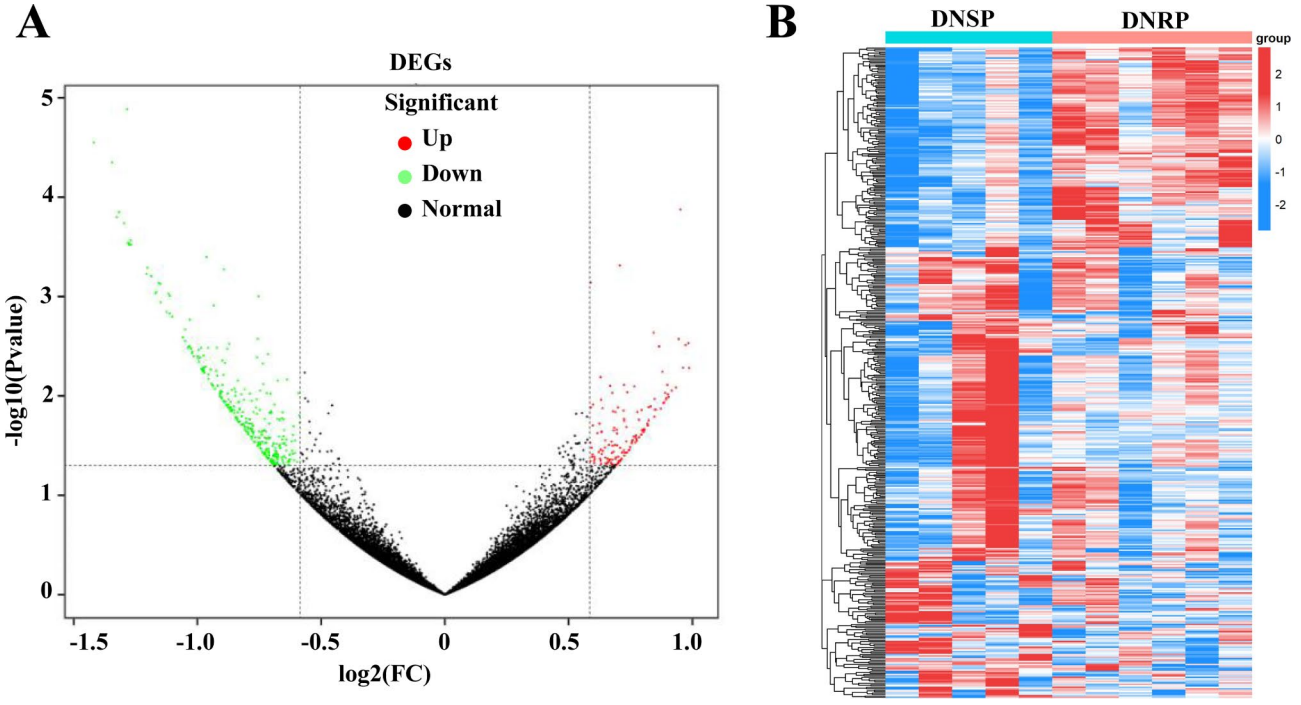

Fig. 5 Differential expression of genes in DNSP vs. DNRP. **A** Volcanic plot of the DEGs. Red: up-regulated; Green: down-regulated; Black: normal. The y axis shows the -log10(*P*- adjusted value). **B** Cluster heatmap of the DEGs

To validate the sequencing results, 5 DEGs from the sequencing results were selected for detection by qRT-PCR. These DEGs include a randomly selected gene COX5A, a ferroptosis-associated gene CCNG2, an autophagy/mitophagy-associated gene RB1CC1, and two apoptosis/necroptosis -associated genes ONT.8101 and ONT.18,929. As shown in Fig. 10, the expression patterns of the four DEGs were consistent with the ONT sequencing results, with the exception of RB1CC1. Compared to the DNSP group, the expression of ONT.8101, CCNG2, and ONT.18,929 were significantly down-regulated in the DNRP group, while COX5A was significantly elevated. These results not only verified the reliability of ONT sequencing results, but also showed that COX5A, ONT.8101, CCNG2, and ONT.18,929 may be related to the rate of DN progression.

Discussion

DN is one of the main causes of end-stage renal disease and has always been a complex worldwide clinical problem. In this study, we used full-length transcriptome sequencing to depict the transcriptome landscape that leads to differences in the fast and slow progression of DN, identifying and characterizing the 1,815 TFs, 45,808 SSRs, 1,050 lncRNA, 341 DETs, and 456 DEGs that may be involved. Importantly, based on the functional analysis of DETs, we found that ferroptosis-related pathways oxidative phosphorylation, iron ion binding, and mitophagy may mediate the fast and slow progression of DN. Moreover, Functional analysis of DEGs suggests that DEGs may determine the rate of DN progression through pathways such as ferroptosis, autophagy/mitophagy, apoptosis/necroptosis, and lipid metabolism.

TFs family E2F has been shown to be involved in DN, such as the transcription factor E2F3. Increasingly studies pursued the potential mechanism of DN pathogenesis and confirmed that E2F3 regulation plays a crucial role in DN. For example, a previous study revealed that up-regulating miR-503 expression promoted podocyte injury via targeting E2F3 in DN [30]. Another finding indicated that the high expression of miR-770-5p stimulated podocyte injury by targeting E2F3 to involve in DN progression [31]. Furthermore, overexpression of MIAT accelerated mesangial cell proliferation and fibrosis by sponging miR-147a and regulating E2F3 [32]. Similar to these findings, we identified that the transcription factor E2F may be involved in DN progression. Moreover, we also identified some TFs not previously reported to be associated with DN, such as zf-C2H2 and ZBTB. These TFs may also affect the development of DN but it still needs more effort for future DN research.

In recent years, there have been many studies on the relationship between ferroptosis and DN. For instance, Jin et al. revealed that umbelliferone suppressed ferroptosis induced by high glucose via activating the Nrf2/HO-1 pathway to relieve DN progression [33]. Glab protected the kidney of diabetic rats may be through the inhibition of ferroptosis and VEGF/Akt/ERK signaling pathway

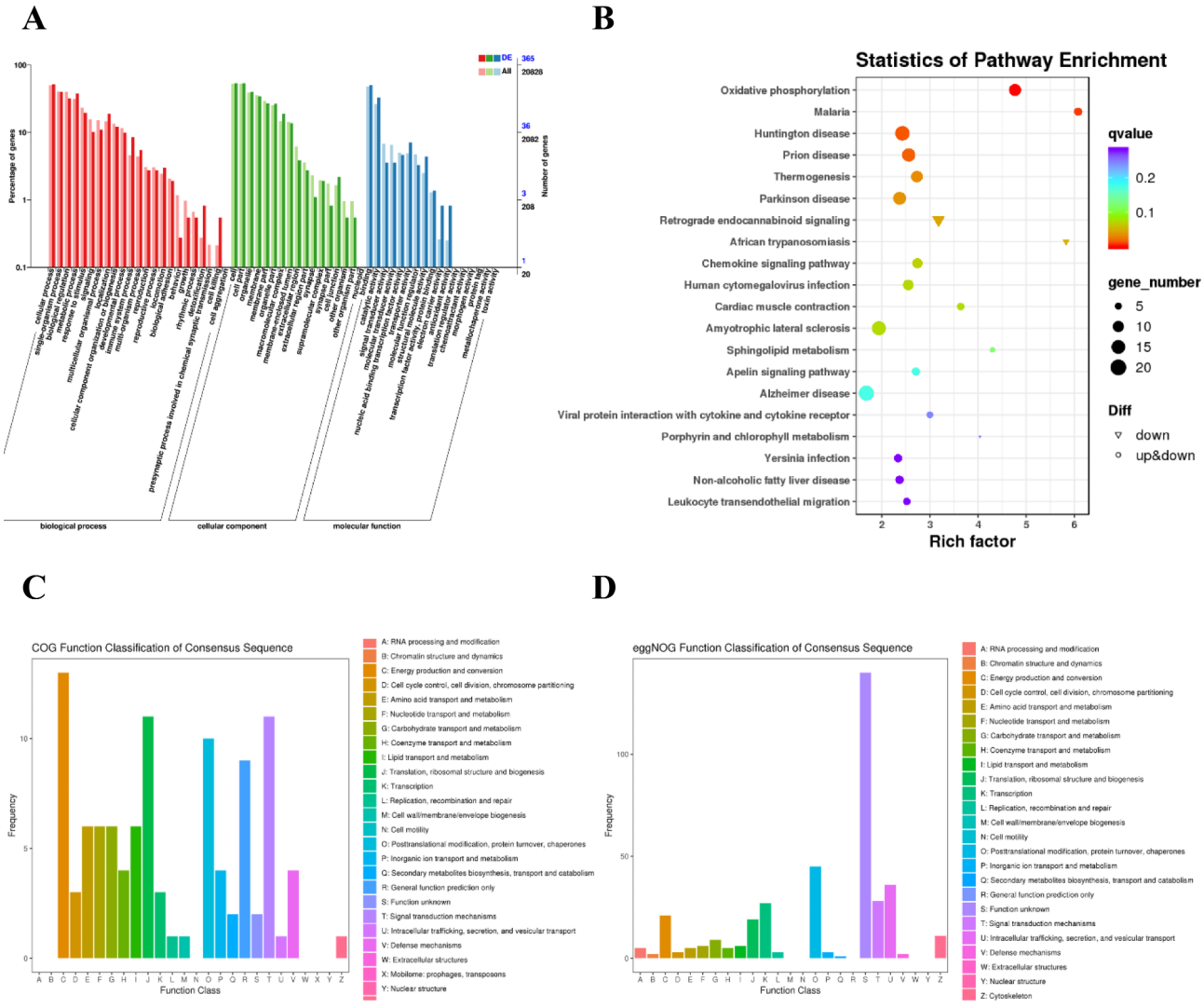

Fig. 6 Functional annotation of DEGs. **A** Annotation of GO function. **B** Bubble plot of KEGG signaling pathway enrichment. **C** Annotation of COG function. **D** Annotation of eggNOG function

[34]. Meanwhile, recent reports suggested that mmu_circRNA_0000309 is involved in Germacrone-mediated improvement of DN through regulating ferroptosis by targeting miR-188-3p/GPX4 signaling axis [35]. Similarly, our results also pointed out that ferroptosis may be involved in the pathogenesis of DN, and many DEGs that were involved in ferroptosis were identified, including MMD [36], ZEB1 [37], PCBP1 [38], and NF2 [39]. In addition, it is well known that SLC7A11 is the classical ferroptosis marker gene, and other members of the SLC family including SLC1A5, SLC3A2, SLC38A1, SLC1A5, and SLC39A14 have also been reported to be possibly associated with ferroptosis [40, 41]. Interestingly, we identified 7 SLC family members of DEGs, SLC4A1, SLC38A5, SLC25A40, SLC12A7, SLC16A7, SLC35E1, and SLC47A1, in the DNSP and DNRP comparison groups. Although their involvement in ferroptosis has not yet been reported, given our current incomplete understanding of the SLC family and the large number of SLC family members involved in ferroptosis, we venture to guess that these 7 SLC family members may also be involved in the rate of DN progression through ferroptosis or some other pathway.

Moreover, autophagy/mitophagy and apoptosis/necroptosis are significant pathways in the DN, and a large number of studies support this. For example, PACS-2 ameliorated renal tubular injury in DN by promoting mitochondria-associated endoplasmic reticulum membrane formation and mitophagy [42]. Disrupting PHB2-mediated mitophagy by TIPE1 up-regulating in the tubular epithelial cell lead to aggravating DN [43]. Sar improved DN by targeting the GSK3β pathway and stimulating podocyte autophagy [44]. Apoptosis/necroptosis participated in DN through many different pathways has

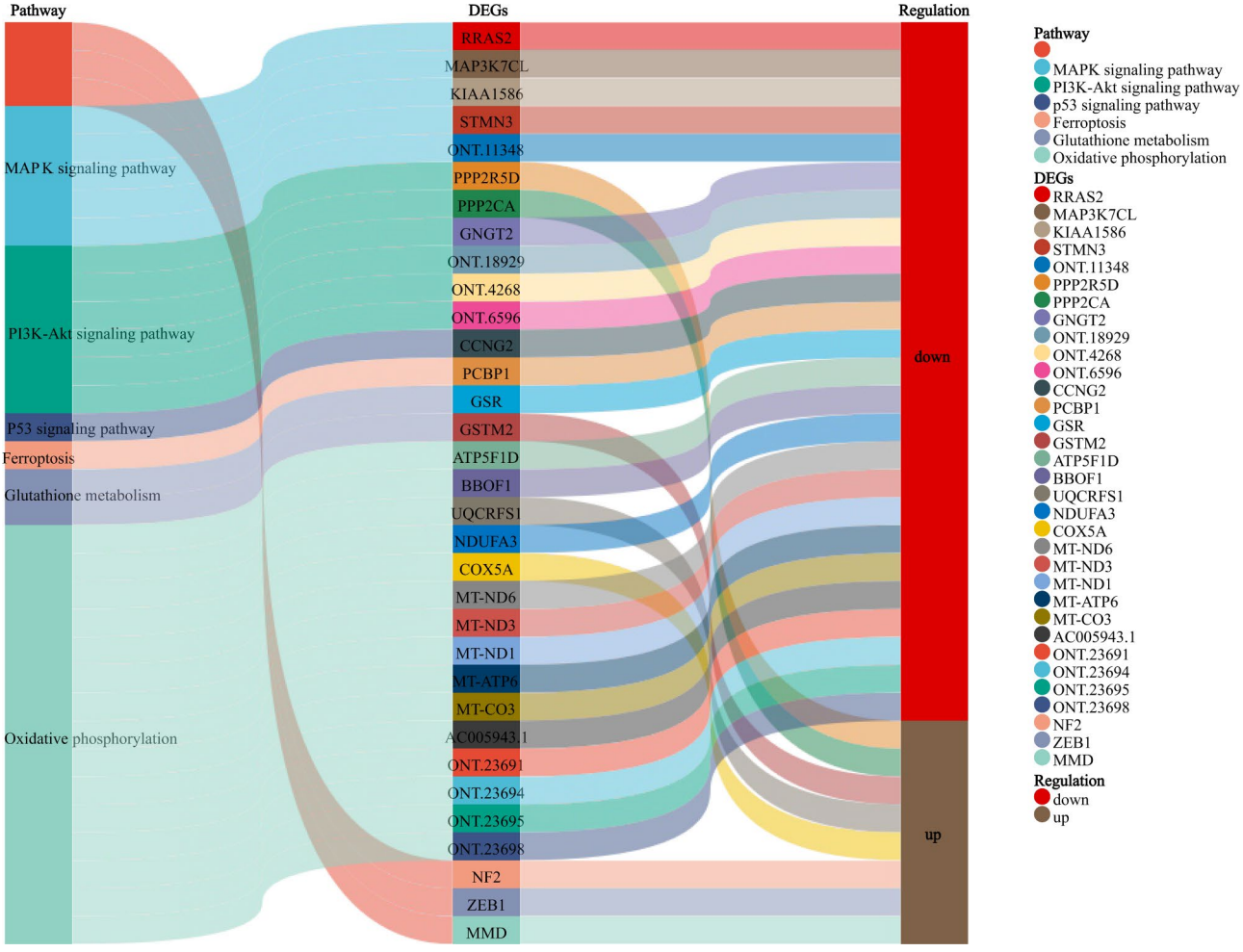

Fig. 7 Sankey diagram of ferroptosis-related DEGs in DNSP vs. DNRP

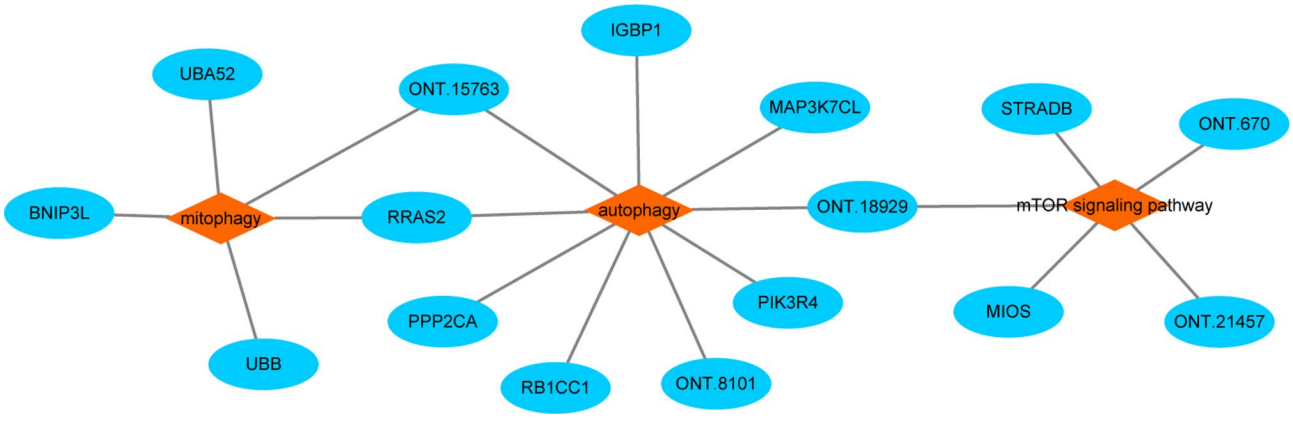

Fig. 8 Network diagram of autophagy/mitophagy-related DEGs

also been reported, such as p38 MAPK or mTOR signaling pathway [24] or RIP-1/RIP-3-p-p38MAPK signaling pathway [28] In our study, autophagy/mitophagy and apoptosis/necroptosis related DEGs were also identified, and they may play an important in the rate of DN progression. However, the specific mechanism of these DEGs in DN is still unclear, and further studies are needed to determine the pathogenesis.

Our results indicated that oxidative phosphorylation, primary immunodeficiency, and sphingolipid metabolism may be involved in DN, and past research backed this up. For example, the substantial contribution of

Table 2 Apoptosis/necroptosis pathway enriched DEGs

Gene	DNSP (Mean CPM)	DNRP (Mean CPM)	log2(FC)	*p*-value
ONT.18,929	2.58668	0.984233	-0.892577	0.01145690
ONT.3200	5.06372	24.3465	0.945025	0.00268157
H2AFV	92.5562	54.1733	-0.767248	0.0263310
CAMK2D	10.9294	8.86908	-0.657166	0.0442141
NLRP3	4.32186	11.2620	0.597650	0.0199185
ONT.8101	3.10668	1.39987	-1.15754	0.000728629

oxidative stress in DN has been summarized in a review by Kashihara et al. [45] and Singh et al. [46]. Other results suggested that diabetes impaired epithelial immunity as a consequence of chronic and inappropriate activation of anti-regulatory immune responses [47]. The early intervention of mesenchymal stem cells can prevent renal injury through immune regulation of diabetes rats, thereby restoring the homeostasis of the immune microenvironment and helping to prevent renal dysfunction and glomerulosclerosis [48]. Previous studies have shown that there is an association between the elevated level of glycosphingolipids and DN [49–51]. Lopes-Virella et al. pointed out that the decrease of long and very long lactosylceramides could predict the development of macroalbuminuria in type 1 diabetes [51] and urinary ceramides might be associated with the pathological condition of DN [52]. Therefore, we suggest that in the future more efforts should be invested in the study of oxidative phosphorylation, primary immunodeficiency, and sphingolipid metabolism in DN progression.

We obtained hub genes (HBB-206, CD163-209, HBA1-201, HSPA1A, and AHSP-201) through the PPI network. Among them, CD163 and HSPA1A have been reported to be associated with DN progression. For example, soluble plasma protein CD163 could be served as early biomarker of DN in Swedish [53]. HSPA1A, the stress response gene, expression was increased in diabetic mice with kidney injury, but reduced after hyperbaric oxygen therapy [54].

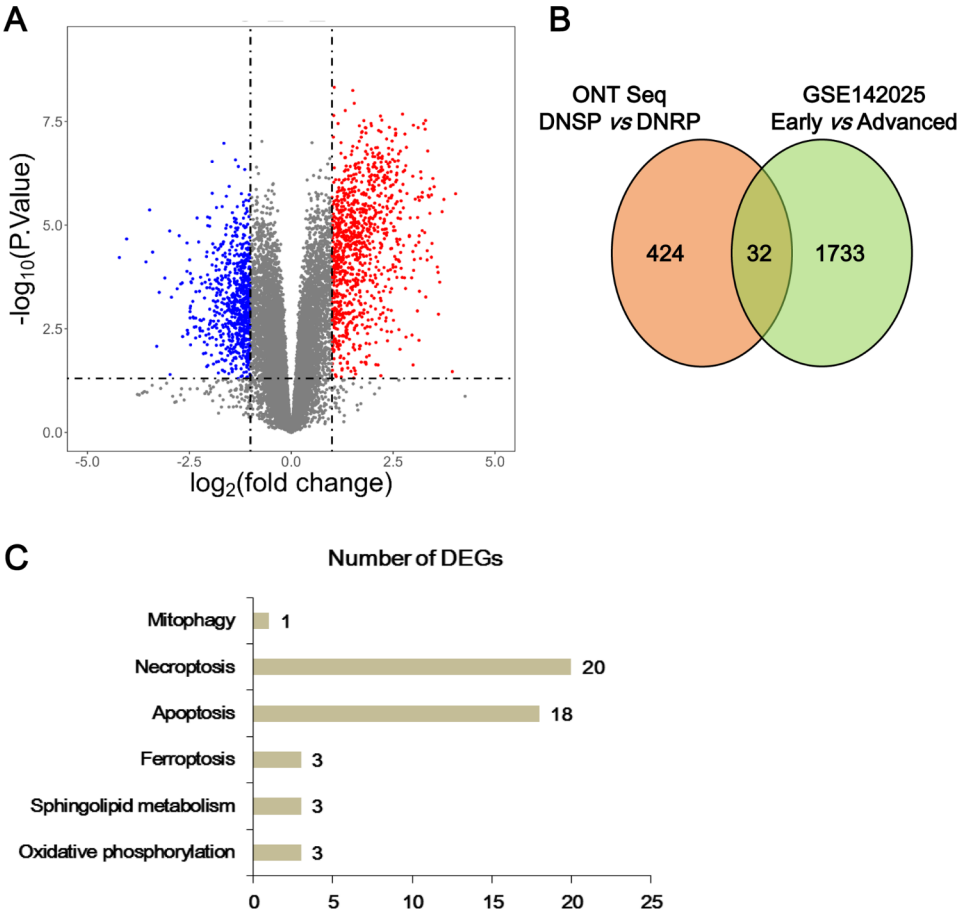

Fig. 9 DEGs in GSE142025 dataset. **A** Volcanic plot of the DEGs. Red and blue dots mean up-regulated and down-regulated DEGs in the advanced DN group compared with the early DN group, respectively. **B** Venn diagram shows the DEGs that are shared in ONT sequencing and GSE142025 dataset. **C** Bar graph of DEGs enriched in pathways of mitophagy, necroptosis, apoptosis, ferroptosis, sphingolipid metabolism, and oxidative phosphorylation in the GSE142025 dataset

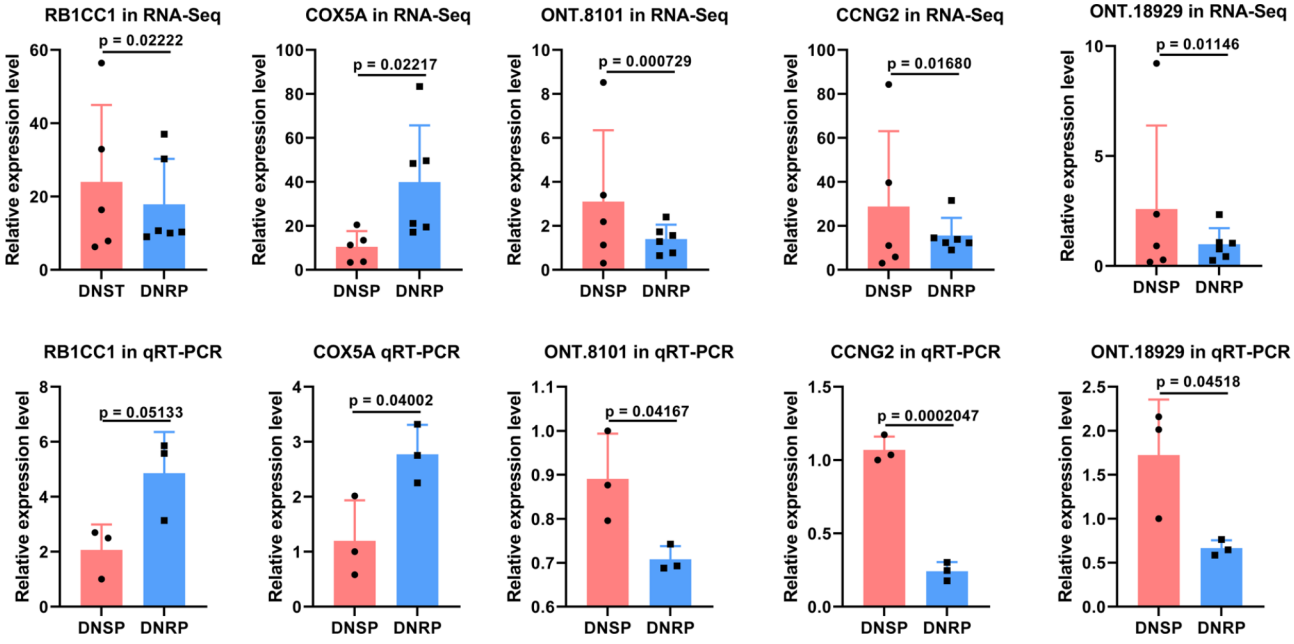

Fig. 10 Validation by qRT-PCR. t test, a *p*-value of less than 0.05 was considered statistically significant

However, the role of the remaining hub gene in DN has not yet been reported, which urges us to follow up with in-depth studies in this area.

Conclusions

In summary, we obtained the full-length transcripts by ONT sequencing technology and ascertained the structural analysis and functional annotation of novel transcripts. A total of 46,250 nonredundant transcript sequences and 22,682 novel transcripts were obtained. Afterward, we predicted 45,808 SSRs, 1,815 transcription factors, 5,993 complete ORFs, and 1,050 lncRNA from the new transcripts. The hub genes may be the critical genes regulating the progression of DN, including HBB, CD163, HBA1, HSPA1A, and AHSP. Furthermore, DETs may be involved in the determination of DN progression rate through signaling pathways such as oxidative phosphorylation, iron ion binding, and mitophagy. Functional analysis of DEGs suggests that DEGs may determine the rate of DN progression through pathways such as ferroptosis, autophagy/mitophagy, apoptosis/necroptosis, and lipid metabolism. Our findings may help to understand the regulatory mechanisms underlying the differences in the fast and slow progression of DN.

Abbreviations

DN	Diabetic nephropathy
DNSP	DN patients with slow progression
DNRP	DN patients with rapid progression
DETs	differentially expressed transcripts
DEGs	differentially expressed genes
ESRD	end-stage renal disease
RAAS	renin–angiotensin–aldosterone system
TNF-α	tumor necrosis factor-α
IL-6	including interleukin-6
IL-10	interleukin-10
ONT	Oxford Nanopore Technologies
AS	alternative splicing
SSR	Simple sequence repeat
MISA	multiple intelligent software agents
CDS	coding sequence
TF	Transcription factors
TFDB	transcription factor binding site
GO	Gene Ontology
KEGG	Kyoto Encyclopedia of Genes and Genomes
KOBAS	KO-Based Annotation System
COG	Clusters of Orthologous Groups
GSEA	Gene set enrichment analysis
PPI	Protein-protein interaction
qRT-PCR	Quantitative Real-Time PCR

Supplementary Information

The online version contains supplementary material available at https://doi.org/10.1186/s12920-024-02006-2.

Supplementary Material 1.

Supplementary Material 2.

Supplementary Material 3.

Supplementary Material 4.

Supplementary Material 5.

Supplementary Material 6.

Acknowledgements

Not applicable.

Authors' contributions

EJ: Conceptualization, Validation, and Writing – original draft; LSY: Conceptualization, Validation, and Writing – original draft; MDN: Funding acquisition, Conceptualization, and Writing – original draft; ZGQ: Data curation, Visualization, and Writing – original draft; CSL: Formal analysis, and Writing – original draft; LB: Investigation, and Writing – original draft; LXH: Methodology,

and Writing – review & editing; LHY: Funding acquisition, and Writing – review & editing; BL: Project administration, and Writing – review & editing; LXM: Resources, and Writing – review & editing; FRG: Conceptualization, and Writing – review & editing; ZYL: Conceptualization, Supervision, Funding acquisition, and Writing – review & editing. All authors read and approved the final version of the manuscript.

Funding
This study was supported by the National Natural Science Foundation of China [81860136, 82460146], Key Research and Development Programs in Ningxia Hui Autonomous Region [2022BEG03121], National Natural Science Foundation of Ningxia Hui Autonomous Region [2022AAC02059; 2022AAC03379; 2021AAC03311].

Availability of data and materials
Sequence data that support the findings of this study have been deposited in the National Center for Biotechnology Information (https://www.ncbi.nlm.nih.gov/) with the primary accession code PRJNA1148683.

Declarations

Ethics approval and consent to participate
This study was approved by the Ethics Committee of People's Hospital of Ningxia Hui Autonomous Region, approval number [2021]-ZDYF-040, and was based on the Declaration of Helsinki as the moral principle. Informed consent of all patients was obtained for this study.

Consent for publication
Not applicable.

Competing interests
The authors declare no competing interests.

Author details
[1]Department of Nephrology, People's Hospital of Ningxia Hui Autonomous Region, People's Hospital of Ningxia Hui Autonomous Region, No.157, West 5th Road, Yinchuan 750002, China
[2]Department of clinical medicine, Xi'an Jiaotong University, Xi'an, China
[3]The Third Clinical Medical College of Ningxia Medical University, Yinchuan, China
[4]Department of Geriatrics, People's Hospital of Ningxia Hui Autonomous Region, Yinchuan, China
[5]Department of Nephrology, The Second Affiliated Hospital of Xi'an Jiaotong University, Xi'an, China
[6]Department of Nephrology, The First Affiliated Hospital of Shandong First Medical University & Shandong Provincial Qianfoshan Hospital, Shandong Institute of Nephrology, Jinan, China
[7]Department of Nephrology, Chengdu first people's hospital, Chengdu, Sichuan 610000, China

Received: 17 November 2023 / Accepted: 5 September 2024
Published online: 08 October 2024

References

1. Himmelfarb J, Tuttle K. New therapies for diabetic kidney disease. N Engl J Med. 2013;369(26):2549–50.
2. Long J, Badal S, Ye Z, Wang Y, Ayanga B, Galvan D, Green N, Chang B, Overbeek P, Danesh F. Long noncoding RNA Tug1 regulates mitochondrial bioenergetics in diabetic nephropathy. J Clin Investig. 2016;126(11):4205–18.
3. Gheith O, Farouk N, Nampoory N, Halim M, Al-Otaibi T. Diabetic kidney disease: world wide difference of prevalence and risk factors. J Nephropharmacology. 2016;5(1):49–56.
4. Guo J, Liu Z, Gong R. Long noncoding RNA: an emerging player in diabetes and diabetic kidney disease. Clin Sci (London, England: 1979). 2019;133(12):1321–39.
5. Jeong K, Lee T, Ihm C, Lee S, Moon J, Lim S. Effects of sildenafil on oxidative and inflammatory injuries of the kidney in streptozotocin-induced diabetic rats. Am J Nephrol. 2009;29(3):274–82.
6. Forbes J, Coughlan M, Cooper M. Oxidative stress as a major culprit in kidney disease in diabetes. Diabetes. 2008;57(6):1446–54.
7. Lim A, Tesch G. Inflammation in diabetic nephropathy. Mediat Inflamm. 2012;2012:146154.
8. Shikata K, Makino H. Microinflammation in the pathogenesis of diabetic nephropathy. J Diabetes Invest. 2013;4(2):142–9.
9. Hameed I, Masoodi S, Malik P, Mir S, Ghazanfar K, Ganai B. Genetic variations in key inflammatory cytokines exacerbates the risk of diabetic nephropathy by influencing the gene expression. Gene. 2018;661:51–9.
10. Qin S, Jiang H, Lu D, Zhou Y. Association of interleukin-10 polymorphisms with risk of irritable bowel syndrome: a meta-analysis. World J Gastroenterol. 2013;19(48):9472–80.
11. Deamer D, Akeson M, Branton D. Three decades of nanopore sequencing. Nat Biotechnol. 2016;34(5):518–24.
12. Magi A, Semeraro R, Mingrino A, Giusti B, D'Aurizio R. Nanopore sequencing data analysis: state of the art, applications and challenges. Brief Bioinform. 2018;19(6):1256–72.
13. Krishnakumar R, Sinha A, Bird S, Jayamohan H, Edwards H, Schoeniger J, Patel K, Branda S, Bartsch M. Systematic and stochastic influences on the performance of the MinION nanopore sequencer across a range of nucleotide bias. Sci Rep. 2018;8(1):3159.
14. Xue X, Yu J, Li C, Wang F, Guo Y, Li Y, Shi H. Full-length transcriptome sequencing analysis of differentially expressed genes and pathways after treatment of Psoriasis with Oxymatrine. Front Pharmacol. 2022;13:889493.
15. Oehler D, Spychala A, Gödecke A, Lang A, Gerdes N, Ruas J, Kelm M, Szendroedi J, Westenfeld R. Full-length transcriptomic analysis in murine and human heart reveals diversity of PGC-1α promoters and isoforms regulated distinctly in myocardial ischemia and obesity. BMC Biol. 2022;20(1):169.
16. Liu J, Zhang X, Xu G. Clinical efficacy, safety, and cost of nine Chinese patent medicines combined with ACEI/ARB in the treatment of early diabetic kidney disease: a network meta-analysis. Front Pharmacol. 2022;13:939488.
17. Ma X, Ma J, Leng T, Yuan Z, Hu T, Liu Q, Shen T. Advances in oxidative stress in pathogenesis of diabetic kidney disease and efficacy of TCM intervention. Ren Fail. 2023;45(1):2146512.
18. Jin B, Liu J, Zhu Y, Lu J, Zhang Q, Liang Y, Shao Q, Jiang C. Kunxian capsule alleviates podocyte injury and proteinuria by inactivating β-catenin in db/db mice. Front Med (Lausanne). 2023;10:1213191.
19. Lu M, Ou J, Deng X, Chen Y, Gao Q. Exploring the pharmacological mechanisms of Tripterygium wilfordii against diabetic kidney disease using network pharmacology and molecular docking. Heliyon. 2023;9(6):e17550.
20. Pfaffl MW. A new mathematical model for relative quantification in real-time RT-PCR. Nucleic Acids Res. 2001;29(9):e45.
21. Li Q, Liao J, Chen W, Zhang K, Li H, Ma F, Zhang H, Han Q, Guo J, Li Y, Hu L, Pan J, Tang Z. NAC alleviative ferroptosis in diabetic nephropathy via maintaining mitochondrial redox homeostasis through activating SIRT3-SOD2/Gpx4 pathway. Free Radic Biol Med. 2022;187:158–70.
22. Dixon S, Lemberg K, Lamprecht M, Skouta R, Zaitsev E, Gleason C, Patel D, Bauer A, Cantley A, Yang W. Morrison B and Stockwell B. Ferroptosis: an iron-dependent form of nonapoptotic cell death. Cell. 2012;149(5):1060–72.
23. Su L, Zhang J, Gomez H, Kellum JA, Peng Z. Mitochondria ROS and mitophagy in acute kidney injury. Autophagy. 2023;19(2):401–14.
24. Song S, Qiu D, Wang Y, Wei J, Wu H, Wu M, Wang S, Zhou X, Shi Y, Duan H. TXNIP deficiency mitigates podocyte apoptosis via restraining the activation of mTOR or p38 MAPK signaling in diabetic nephropathy. Exp Cell Res. 2020;388(2):111862.
25. Huang C, Zhang Y, Kelly D, Tan C, Gill A, Cheng D, Braet F, Park J, Sue C, Pollock C, Chen X. Thioredoxin interacting protein (TXNIP) regulates tubular autophagy and mitophagy in diabetic nephropathy through the mTOR signaling pathway. Sci Rep. 2016;6:29196.
26. Wu X, Zheng Y, Liu M, Li Y, Ma S, Tang W, Yan W, Cao M, Zheng W, Jiang L, Wu J, Han F, Qin Z, Fang L, Hu W, Chen Z, Zhang X. BNIP3L/NIX degradation leads to mitophagy deficiency in ischemic brains. Autophagy. 2021;17(8):1934–46.
27. Popelka H, Klionsky D. The RB1CC1 claw-binding motif: a new piece in the puzzle of autophagy regulation. Autophagy. 2022;18(2):237–9.
28. Al Shahrani M, Chandramoorthy H, Alshahrani M, Abohassan M, Eid R, Ravichandran K, Rajagopalan P. Cassia auriculata leaf extract ameliorates diabetic nephropathy by attenuating autophagic necroptosis via RIP-1/RIP-3-p-p38MAPK signaling. J Food Biochem. 2021;45(7):e13810.
29. Wang B, Cui Y, Zhang Q, Wang S, Xu S. Selenomethionine alleviates LPS-induced JNK/NLRP3 inflammasome-dependent necroptosis by modulating miR-15a and oxidative stress in chicken lungs. Metallomics. 2021;13(8):mfab048.

30. Zha F, Bai L, Tang B, Li J, Wang Y, Zheng P, Ji T, Bai S. MicroRNA-503 contributes to podocyte injury via targeting E2F3 in diabetic nephropathy. J Cell Biochem. 2019;120(8):12574–81.
31. Guo J, Han J, Liu J, Wang S. MicroRNA-770-5p contributes to podocyte injury via targeting E2F3 in diabetic nephropathy. Brazilian J Med Biol Res = Revista brasileira de pesquisas medicas e Biologicas. 2020;53(9):e9360.
32. Ji T, Qi Y, Li X, Tang B, Wang Y, Zheng P, Li W, Qu X, Feng L, Bai S. Loss of lncRNA MIAT ameliorates proliferation and fibrosis of diabetic nephropathy through reducing E2F3 expression. J Cell Mol Med. 2020;24(22):13314–23.
33. Jin T, Chen C. Umbelliferone delays the progression of diabetic nephropathy by inhibiting ferroptosis through activation of the Nrf-2/HO-1 pathway. Food Chem Toxicology: Int J Published Br Industrial Biol Res Association. 2022;163:112892.
34. Tan H, Chen J, Li Y, Li Y, Zhong Y, Li G, Liu L, Li Y. Glabridin, a bioactive component of licorice, ameliorates diabetic nephropathy by regulating ferroptosis and the VEGF/Akt/ERK pathways. Mol Med (Cambridge Mass). 2022;28(1):58.
35. Jin J, Wang Y, Zheng D, Liang M, He QA, Novel Identified Circular RNA. mmu_mmu_circRNA_0000309, involves in germacrone-mediated improvement of Diabetic Nephropathy through regulating ferroptosis by targeting miR-188-3p/GPX4 Signaling Axis. Antioxid Redox Signal. 2022;36:740–59.
36. Phadnis VV, Snider J, Wong V, Vaccaro KD, Kunchok T, Allen J, Yao Z, Geng B. Weiskopf K and Stagljar I. MMD scaffolds ACSL4 and MBOAT7 to promote polyunsaturated phospholipid synthesis and susceptibility to ferroptosis. bioRxiv. 2022; preprint.
37. Wang X, Liu M, Chu Y, Liu Y, Cao X, Zhang H, Huang Y, Gong A, Liao X, Wang D, Zhu H. O-GlcNAcylation of ZEB1 facilitated mesenchymal pancreatic cancer cell ferroptosis. Int J Biol Sci. 2022;18(10):4135–50.
38. Yue L, Luo Y, Jiang L, Sekido Y, Toyokuni S. PCBP2 knockdown promotes ferroptosis in malignant mesothelioma. Pathol Int. 2022;72(4):242–51.
39. Wu J, Minikes AM, Gao M, Bian H, Li Y, Stockwell BR, Chen ZN, Jiang X. Intercellular interaction dictates cancer cell ferroptosis via NF2-YAP signalling. Nature. 2019;572(7769):402–6.
40. Zhao J, Wang Y, Tao L, Chen L. Iron transporters and ferroptosis in malignant brain tumors. Front Oncol. 2022;12:861834.
41. Chen X, Li J, Kang R, Klionsky DJ, Tang D. Ferroptosis: machinery and regulation. Autophagy. 2021;17(9):2054–81.
42. Li C, Li L, Yang M, Yang J, Zhao C, Han Y, Zhao H, Jiang N, Wei L, Xiao Y, Liu Y, Xiong X, Xi Y, Luo S, Deng F, Chen W, Yuan S, Zhu X, Xiao L, Sun L. PACS-2 ameliorates tubular Injury by facilitating endoplasmic reticulum-mitochondria contact and Mitophagy in Diabetic Nephropathy. Diabetes. 2022;71(5):1034–50.
43. Liu L, Bai F, Song H, Xiao R, Wang Y, Yang H, Ren X, Li S, Gao L, Ma C, Yang X, Liang X. Upregulation of TIPE1 in tubular epithelial cell aggravates diabetic nephropathy by disrupting PHB2 mediated mitophagy. Redox Biol. 2022;50:102260.
44. Li X, Jiang H, Xu L, Liu Y, Tang J, Shi J, Yu X, Wang X, Du L, Lu Q, Li C, Liu Y, Yin X. Sarsasapogenin restores podocyte autophagy in diabetic nephropathy by targeting GSK3β signaling pathway. Biochem Pharmacol. 2021;192:114675.
45. Kashihara N, Haruna Y, K Kondeti V, Kanwar S. Oxidative stress in diabetic nephropathy. Curr Med Chem. 2010;17(34):4256–69.
46. Singh DK, Winocour P, Farrington K. Oxidative stress in early diabetic nephropathy: fueling the fire. Nat Rev Endocrinol. 2011;7(3):176–84.
47. Chen N, Chong T, Loh H, Lim K, Gan V, Wang M, Kon O. Negative regulatory responses to metabolically triggered inflammation impair renal epithelial immunity in diabetes mellitus. J Mol Med. 2013;91(5):587–98.
48. Li Y, Liu J, Liao G, Zhang J, Chen Y, Li L, Li L, Liu F, Chen B, Guo G, Wang C, Yang L, Cheng J, Lu Y. Early intervention with mesenchymal stem cells prevents nephropathy in diabetic rats by ameliorating the inflammatory microenvironment. Int J Mol Med. 2018;41(5):2629–39.
49. Zhang X, Kiechle F, Review. Glycosphingolipids in health and disease. Ann Clin Lab Sci. 2004;34(1):3–13.
50. Subathra M, Korrapati M, Howell L, Arthur J, Shayman J, Schnellmann R, Siskind L. Kidney glycosphingolipids are elevated early in diabetic nephropathy and mediate hypertrophy of mesangial cells. Am J Physiol Renal Physiol. 2015;309(3):F204-15.
51. Lopes-Virella M, Baker N, Hunt K, Hammad S, Arthur J, Virella G, Klein R. Glycosylated sphingolipids and progression to kidney dysfunction in type 1 diabetes. J Clin Lipidol. 2019;13(3):481-e4911.
52. Morita Y, Kurano M, Sakai E, Nishikawa T, Nishikawa M, Sawabe M, Aoki J, Yatomi Y. Analysis of urinary sphingolipids using liquid chromatography-tandem mass spectrometry in diabetic nephropathy. J Diabetes Invest. 2020;11(2):441–9.
53. Samuelsson M, Dereke J, Svensson MK, Landin-Olsson M, Hillman M, on the behalf of the DSg. Soluble plasma proteins ST2 and CD163 as early biomarkers of nephropathy in Swedish patients with diabetes, 15–34 years of age: a prospective cohort study. Diabetol Metab Syndr. 2017;9:41.
54. Verma R, Chopra A, Giardina C, Sabbisetti V, Smyth JA, Hightower LE, Perdrizet GA. Hyperbaric oxygen therapy (HBOT) suppresses biomarkers of cell stress and kidney injury in diabetic mice. Cell Stress Chaperones. 2015;20(3):495–505.

Publisher's note